

Resource Optimization with Flexible Numerology and Frame Structure for Heterogeneous Services

Lei You¹, Qi Liao², Nikolaos Pappas³, and Di Yuan³

¹Department of Information Technology, Uppsala University, Sweden

²Nokia Bell Labs, Stuttgart, Germany

³Department of Science and Technology, Linköping University, Sweden

{lei.you}@it.uu.se qi.liao@nokia-bell-labs.com {nikolaos.pappas, di.yuan}@liu.se

Abstract—We explore the potential of optimizing resource allocation with flexible numerology in frequency domain and variable frame structure in time domain, in presence of services with different types of requirements. We prove the NP-hardness of the problem, and propose a scalable optimization algorithm based on linear programming and Lagrangian duality. Numerical results show significant advantages of adopting flexibility in both time and frequency domains for capacity enhancement and meeting the requirements of mission critical services.

I. INTRODUCTION

The fifth generation (5G) of wireless communications systems is required to support a large variety of services [1]. A promising solution for higher resource efficiency while providing lower latency is the scalable transmission time intervals (TTIs) [2]–[7]. These works fall within the general notion of flexible resource allocation in the time-frequency domain, Optimization along the frequency dimension yields similar structures to problems such as multi-dimensional KNAPSACK or weighted MATCHING [8]. Resource optimization adopting flexibility in both dimensions regarding frequency and time, named *2-dimensional (2-D) resource allocation*, poses new challenges [9], [10]. Although flexible resource allocation along both the time and frequency dimensions is not new [9]–[15], *from an integer programming point of view, frequency selective resource allocation with flexible sizes of resource units along both the frequency and time dimensions*, has not yet been addressed to the best of our knowledge.

Based on 3GPP release for scalable numerologies and frame structures [16], we consider the resulting 2-D resource allocation problem. We address tractability and propose *an algorithm with scalability*, utilizing both the *primal* space and *dual* space of optimization. We then provide numerical results for performance assessment.

II. SYSTEM MODEL

Consider a base station and two categories of services. The first category, denoted by $\mathcal{K}^{(\ell)}$, has strict latency requirement. For any service $k \in \mathcal{K}^{(\ell)}$, denote its data demand by q_k (in bits) that has to be met with a latency tolerance of τ_k . Here, the latency tolerance refers to the time until the data has been fully transmitted by the scheduler. The parameter can be set to also account for queueing delay that has taken place, along with the time at the receiver for processing/computing, to meet the overall deadline of delivery. The second category of services is denoted by $\mathcal{K}^{(c)}$, for which the target is to maximize the throughput. For services in $\mathcal{K}^{(c)}$, full buffer is assumed. Moreover, services in $\mathcal{K}^{(\ell)}$ are prioritized over those in $\mathcal{K}^{(c)}$. We define $\mathcal{K} = \mathcal{K}^{(\ell)} \cup \mathcal{K}^{(c)}$ the set of all services.

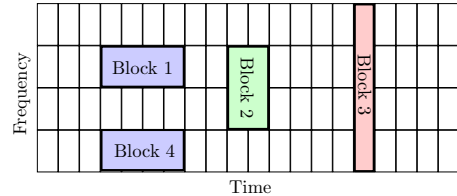


Figure 1. An illustration of resource allocation with three types of blocks. A rectangle of the grid is a basic unit of the resource. A service is allocated with one or multiple blocks, and each block can be assigned to up to one service. Note that blocks 1 and 4 are different blocks with the same shape.

In 5G new radio (NR), a numerology is defined by sub-carrier spacing (SCS) and cyclic prefix (CP) length (a.k.a. the “guard interval” between the symbols). The radio frame structure is characterized by number of slots within a frame. A TTI can consist of one mini-slot with 1-13 symbols supported, or one slot with 14 symbols (or 12 symbols in case of extended CP), or multiple slots if slot aggregation is supported. One resource allocation to a service involves a set of adjacent SCSs and TTIs in the frequency and time domain respectively with a configured CP length. For simplicity, hereafter we refer to the resource configuration of numerology and frame structure as *blocks*, and consider a candidate set \mathcal{B} of blocks, see Figure 1. For each $b \in \mathcal{B}$, the achieved throughput on block b if b is assigned to service k ($k \in \mathcal{K}$) is denoted by $r_{b,k}$.

Given the channel profile, the transmission power, and the noise power, $r_{b,k}$ depends on the configuration of block b , including the time span and frequency range (characterized by SCS and TTI duration), CP length, and symbol duration. Moreover, this rate shall take into account the effect of guardband. To compute the achieved throughput per block, we assume a total number of nine multipath channel profiles [16, Table B.2.1-4], and we predefine the mapping from the configuration parameters to the throughput based on the model in [17]. This model takes into account the inter-symbol-interference (ISI) depending on CP, and approximates the inter-channel interference (ICI) between the neighboring subbands with the same type of numerology (the ICI between subbands with different types of numerologies is not modeled in this paper due to the high complexity). In addition, we also consider the control overhead as one or more consecutive symbols per TTI. Due to limited space, we omit the details but provide the tutorial and source code in IEEE DataPort [18].

III. PROBLEM FORMULATION AND TRACTABILITY

Consider the problem of maximizing the total throughput for $\mathcal{K}^{(c)}$, subject to latency and the demand constraints for $\mathcal{K}^{(\ell)}$.

We use basic unit to refer to the minimum unit of resource in the time-frequency domain in the problem formulation. The set of basic units is denoted by \mathcal{I} . We let $a_{b,i} = 1$ if block b includes basic unit i , otherwise $a_{b,i} = 0$. Recall that a block refers to a rectangular shape located at some specific location in the resource grid, see Figure 1. Taking the figure as an example, there are $20 \times 4 = 80$ basic units. Hence $\mathcal{I} = \{1, \dots, 80\}$. Block 1 is of shape 1×4 , and for this block, $a_{1,i} = 1$ for four elements of \mathcal{I} . Placing this 1×4 shape at all possible positions of the grid, we obtain all blocks and the corresponding a -values for this particular shape. Doing so for all shapes generates the set of all candidate blocks \mathcal{B} . As it can be seen from Figure 1, for each block, the a -values are fully determined by the position of the block and the numerical indexing of the basic units, and the complexity of doing one mapping equals the size of \mathcal{I} , i.e., $|\mathcal{I}|$. The complexity for obtaining all the mappings is $O(|\mathcal{B}||\mathcal{I}|)$. One possible implementation of performing the mapping is detailed in IEEE DataPort [18]. This mapping is done in the pre-processing stage once (not every TTI), and it is totally decoupled from any service to be scheduled, as it only concerns the two sets \mathcal{B} and \mathcal{I} .

The optimization task is to select blocks for each service, such that the latency and demand requirements are met for $\mathcal{K}^{(\ell)}$, without overlapping among chosen blocks. We use optimization variable $x_{b,k} \in \{1, 0\}$ to indicate whether block b ($b \in \mathcal{B}$) is assigned to the service k ($k \in \mathcal{K}$). A block b is infeasible for k ($k \in \mathcal{K}^{(\ell)}$), if the ending time of b exceeds τ_k . This is modeled by setting $r_{b,k} = 0$. The problem is formulated below. The two sets of constraints impose the demand for $\mathcal{K}^{(\ell)}$ and block non-overlapping, respectively.

$$[\text{P0}] \quad \max_{\mathbf{x} \in \{0,1\}} \sum_{b \in \mathcal{B}} \sum_{k \in \mathcal{K}^{(c)}} r_{b,k} x_{b,k} \quad (1a)$$

$$\text{s.t.} \quad \sum_{b \in \mathcal{B}} r_{b,k} x_{b,k} \geq q_k, \quad k \in \mathcal{K}^{(\ell)} \quad (1b)$$

$$\sum_{k \in \mathcal{K}} \sum_{b \in \mathcal{B}} a_{b,i} x_{b,k} \leq 1, \quad i \in \mathcal{I} \quad (1c)$$

Theorem 1: P0 is \mathcal{NP} -hard.

Proof: We construct a polynomial-time reduction from the PARTITION PROBLEM (PP) for a set of integers $\{d_1, \dots, d_n\}$. The task is to determine whether or not there is a partition such that the two subsets have equal sum of $\sum_{i=1}^n d_i/2$, where the numerator is assumed to be even. We define a single TTI size and multiple blocks that take the shape of one basic unit. There are two services, denoted by k^ℓ and k^c , in $\mathcal{K}^{(\ell)}$ and $\mathcal{K}^{(c)}$, respectively. The latency parameter of k^ℓ equals that of the TTI size, and the demand equals $\sum_{i=1}^n d_i/2$. Moreover, $r_{b,1} = r_{b,2} = d_b$, $b = 1, \dots, n$. By construction, (1c) has no effect. Next, one can observe that partitioning the n basic units into two subsets, each providing a total throughput of $\sum_{i=1}^n d_i/2$, is equivalent to a feasible solution to PP. In addition, this can occur if and only if the objective function defined for k^c reaches $\sum_{i=1}^n d_i/2$. Hence the conclusion. ■

IV. PROBLEM SOLVING

We propose a sub-optimal but low-complexity algorithm, consisting in performing assignment of blocks to services, based on utility values generated from *linear programming (LP) relaxation and the Lagrangian dual (LD)*.

A. Block Assignment

We denote by matrix \mathbf{u} of size $|\mathcal{B}| \times |\mathcal{K}|$ the *utility matrix* for all pairs of blocks and services. An element $u_{b,k}$ represents the utility of a block-service pair (b, k) ($b \in \mathcal{B}$ and $k \in \mathcal{K}$). Block assignments for $\mathcal{K}^{(\ell)}$ and $\mathcal{K}^{(c)}$ are treated separately. The former is performed first because of the latency requirement.

Algorithm 1 BA(\mathcal{S}, \mathbf{u}). The input consists of a block-service assignment \mathcal{S} which may be empty, and a utility matrix \mathbf{u} . Set \mathcal{S} is augmented and then returned by the algorithm. We remark that b overlaps with b' if and only if $\exists i \in \mathcal{I} a_{b,i} + a_{b',i} > 1$.

- 1: **repeat**
 - 2: Remove from \mathcal{B} the blocks in \mathcal{S} and those overlapping with the blocks in \mathcal{S} .
 - 3: $(b', k') \leftarrow \arg \max_{b \in \mathcal{B}, k \in \mathcal{K}^{(\ell)}} u_{b,k}$, $\mathcal{S} \leftarrow \mathcal{S} \cup \{(b', k')\}$.
 - 4: **if** $q_{k'}$ is met: $\mathcal{K}^{(\ell)} \leftarrow \mathcal{K}^{(\ell)} \setminus \{k'\}$.
 - 5: **until** $\mathcal{K}^{(\ell)} = \phi$ **or** $\mathcal{B} = \phi$
 - 6: **if** $\mathcal{K}^{(\ell)} \neq \phi$:
 - 7: The demand of the users left in $\mathcal{K}^{(\ell)}$ cannot be met.
 - 8: **repeat**
 - 9: Lines 2–3 with the notation $\mathcal{K}^{(\ell)}$ replaced by $\mathcal{K}^{(c)}$.
 - 10: **until** $\mathcal{B} = \phi$
-

The operations in Lines 2 and 4 cost $O(1)$ by hash-map implementations. By sorting the utilities in advance (which costs $O(|\mathcal{B}||\mathcal{K}^{(\ell)}| \log(|\mathcal{B}||\mathcal{K}^{(\ell)}|))$), along with inspecting the other algorithm operations, one can conclude that the overall complexity is of $O(|\mathcal{B}||\mathcal{K}| \log(|\mathcal{B}||\mathcal{K}|))$.

B. Utility Estimation by LP Relaxation

One way to compute the utility matrix \mathbf{u} is to solve the LP relaxation of P0 and to use the LP optimum \mathbf{x}_{LP} .

$$[\text{P0-LP}] \quad \max_{0 \leq \mathbf{x} \leq 1} \sum_{b \in \mathcal{B}} \sum_{k \in \mathcal{K}^{(c)}} r_{b,k} x_{b,k} \quad \text{s.t. (1b), (1c)} \quad (2a)$$

We denote by $\mathbf{u}_{\text{LP}} = \mathbf{x}_{\text{LP}}$ the LP-based utility. Also, \mathbf{x}_{LP} can be used for initialization: $\mathcal{S} = \{(b, k) : u_{\text{LP},b,k} \geq \rho, b \in \mathcal{B}, k \in \mathcal{K}\}$ with ρ being a threshold.

C. Utility Estimation by LD

By relaxing the constraints (1c) of P0 with Lagrangian multiplier λ_i ($i \in \mathcal{I}$), the Lagrangian is defined as follows:

$$L(\mathbf{x}, \boldsymbol{\lambda}) = \sum_{b \in \mathcal{B}} \sum_{k \in \mathcal{K}^{(c)}} r_{b,k} x_{b,k} + \sum_{i \in \mathcal{I}} \lambda_i \left(1 - \sum_{b \in \mathcal{B}} \sum_{k \in \mathcal{K}} a_{b,i} x_{b,k} \right)$$

The LD function is defined in (3).

$$[\text{P1}] \quad g(\boldsymbol{\lambda}) = \max_{\mathbf{x} \in \{0,1\}} L(\mathbf{x}, \boldsymbol{\lambda}) \quad \text{s.t. (1b)} \quad (3)$$

Accordingly, we have the LD problem:

$$[\text{P0-LD}] \quad \min_{\boldsymbol{\lambda} \geq 0} g(\boldsymbol{\lambda}). \quad (4)$$

We define $\alpha_b = \sum_{i \in \mathcal{I}} \lambda_i a_{b,i}$. Problem P1 decomposes for $\mathcal{K}^{(c)}$ and $\mathcal{K}^{(\ell)}$: The constraints (1b) are only for $\mathcal{K}^{(\ell)}$. There-

fore, solving P1 amounts to solving the two problems P2 and P3 for $\mathcal{K}^{(c)}$ and $\mathcal{K}^{(\ell)}$ respectively, shown below.

$$[\text{P2}] \quad \max_{\mathbf{x}} \sum_{b \in \mathcal{B}} \sum_{k \in \mathcal{K}^{(c)}} (r_{b,k} - \alpha_b) x_{b,k} \quad (5a)$$

$$\text{s.t.} \quad \sum_{k \in \mathcal{K}^{(c)}} x_{b,k} \leq 1, \quad b \in \mathcal{B} \quad (5b)$$

$$x_{b,k} \in \{0, 1\}, \quad b \in \mathcal{B}, \quad k \in \mathcal{K}^{(c)} \quad (5c)$$

$$[\text{P3}] \quad \min_{\mathbf{x} \in \{0,1\}} \sum_{b \in \mathcal{B}} \sum_{k \in \mathcal{K}^{(\ell)}} \alpha_b x_{b,k} \quad (6a)$$

$$\text{s.t.} \quad \sum_{b \in \mathcal{B}} r_{b,k} x_{b,k} \geq q_k, \quad k \in \mathcal{K}^{(\ell)} \quad (6b)$$

Note constraints (5b) are not present in P0, though these are implied by (1c) for services in $\mathcal{K}^{(c)}$. Computing the optimum of P2 is straightforward. Each block b is allocated to the service $\arg \max_k r_{b,k} - \alpha_b$ with $r_{b,k} - \alpha_b > 0$.

Problem P3 further decomposes to $|\mathcal{K}^{(\ell)}|$ problems P3[k] ($k \in \mathcal{K}^{(\ell)}$), each with objective $\max \sum_{b \in \mathcal{B}} \alpha_b x_{b,k}$, constraints $\sum_{b \in \mathcal{B}} r_{b,k} x_{b,k} \geq q_k$, and binary variables $x_{b,k}$ ($b \in \mathcal{B}$).

$$[\text{P3}[k]] \quad \min_{\mathbf{x} \in \{0,1\}} \sum_{b \in \mathcal{B}} \alpha_b x_{b,k} \quad (7a)$$

$$\text{s.t.} \quad \sum_{b \in \mathcal{B}} r_{b,k} x_{b,k} \geq q_k \quad (7b)$$

Each P3[k] can be reformulated as a KNAPSACK PROBLEM, and *optimally* solved by dynamic programming.

The dual problem P0-LD can be solved using a *sub-gradient method* [19]. Denote by $\mathbf{x}_{\text{LD}}^{(h)}$ the LD solution in the h_{th} iteration of the sub-gradient method. We let $\mathbf{u}_{\text{LD}} = \sum_h \mathbf{x}_{\text{LD}}^{(h)}$ to be the LD-based utility.

D. Algorithm Implementation

In addition to $\text{BA}(\mathcal{S}, \mathbf{u}_{\text{LP}})$ and $\text{BA}(\mathcal{S}, \mathbf{u}_{\text{LD}})$, we consider algorithm ‘‘LP+LD’’ that returns the best solution of $\text{BA}(\mathcal{S}, \mathbf{u}_{\text{LP}})$ and $\text{BA}(\mathcal{S}, \mathbf{u}_{\text{LD}})$. We remark that $\text{BA}(\mathcal{S}, \mathbf{u}_{\text{LD}})$ is quite flexible in terms of computational effort, as one can use accumulated \mathbf{u}_{LD} before full convergence. Overall, the algorithm scales well. Moreover, if necessary, the service sets can be decomposed into subsets, and the algorithm can be applied to one subset at a time to further reduce complexity.

V. NUMERICAL RESULTS

The use of flexible numerology is expected to outperform fixed numerology. The purpose of performance evaluation is to examine the amount of improvement, which is of significance in particular as the control channel overhead for supporting the flexible structure is accounted for. The result also tells how well the proposed algorithm is suited for the flexible structure.

Comparing to LTE that applies a fixed SCS of 15 kHz and TTI of 1.0 ms, we consider four shapes, Shape 1, Shape 2, Shape 3, and Shape 4, with SCS being 15 kHz, 30 kHz, 60 kHz, and 60 kHz, CP 4.7 μs , 2.3 μs , 1.2 μs , and 4.17 μs , and the number of symbols 7, 7, 7, and 6, respectively. The TTI durations of the four shapes are 0.5 ms, 0.25 ms, 0.125 ms, and 0.125 ms, respectively. The numerologies ($\Delta f = 2^\mu \times 15$

kHz, $\mu = 0, 1, 2 \dots$) originate from Release 15 [20, Table 4.2-1]. Note that Release 15 also specifies subcarrier spacing up to 240 kHz. However, by [21, Table I], a TTI of 0.125 ms meets all the worst-case transmission latencies for the listed 5G ultra-reliable low-latency communication configurations.

Parameter settings are given in Table I. We test our algorithm for a set of candidate thresholds $\rho \in \{0.05, 0.5, \dots, 0.95\}$ among which the one achieving the best objective is selected. The maximum sub-gradient iterations is set to 200. While calculating the block rates, the impact on capacity due to guardband is included by following the model in [14]. The rate reduction due to control overhead follows that in [22], where two symbols per TTI constitute the overhead. We emphasize on accurate assessment in terms of optimality, that is, how much does the proposed algorithm perform with respect to global optimum. We use the global optimum obtained by solving the integer programming problem (1) via a solver. This is not a scalable method. The purpose here is for benchmarking, to demonstrate that our low-complexity algorithm has little loss in optimality. The number of users as well as the bandwidth is chosen such that the global optimum can be obtained with reasonable amount of computing effort. Similarly, in view of the computational effort of obtaining global optimum for benchmarking, we do not include all TTI sizes that are permitted by 5G NR [20].

Table I
SIMULATION PARAMETERS.

| Parameter | Value |
|--------------------------|--|
| Number of users | 10 with $ \mathcal{K}^{(\ell)} = \mathcal{K}^{(c)} = 5$ |
| Time-frequency domain | 2 ms and 2 MHz |
| SNR range | [5, 30] (dB) |
| Demand q | {16, 32, 64, 128, 256, 512} (kbps) |
| Latency tolerance τ | {0.25, 0.5, 1.0, 1.5, 2} (ms) |
| Threshold (Section IV-B) | $\rho \in \{0.05, 0.1, \dots, 0.95\}$ |

Figure 2 shows the average bit rate of services in $\mathcal{K}^{(c)}$ with respect to the latency tolerance τ of $\mathcal{K}^{(\ell)}$. For the non-flexible structures, Shape 1, Shape 2, and Shape 3 are used separately. Each of these structures is referred to in the format of ‘‘TTI-SCS’’ (e.g. 0.25ms-30kHz means a shape of a fixed TTI of 0.25 ms and a fixed SCS of 30 kHz).

The flexible structure significantly outperforms the non-flexible ones. The system tends to benefit more from flexible structure when the latency tolerance becomes more stringent. Note that our algorithm with flexible structure is near-optimal. Among the three non-flexible schemes, 0.25ms-30kHz outperforms the other two. This result is related to that, in the optimization problem, the throughput of the services in $\mathcal{K}^{(c)}$, is subject to latency constraints of services in $\mathcal{K}^{(\ell)}$. For resource allocation, blocks of 0.5ms-15kHz and 0.125ms-60kHz have low flexibility in the time and frequency domains, respectively. The former does not have many choices in meeting the latency requirements of $\mathcal{K}^{(\ell)}$, leading to poor throughput for $\mathcal{K}^{(c)}$. The latter is not efficient on the frequency domain (due to frequency selectivity), though this inefficiency is mitigated when the latency tolerance is high, as more choices become available in the time domain. Blocks of 0.25ms-30kHz strikes a balance between short TTI size (to meet latency-constrained services) and flexibility in the frequency domain.

Without showing by the figures, we remark that the problem feasibility of the three non-flexible schemes is very sensitive

to the latency tolerance. This issue is alleviated by the flexible structure. In comparison to the related work [23] considering advantages of flexible numerology, our results emphasize the significance of block-service assignment optimization.

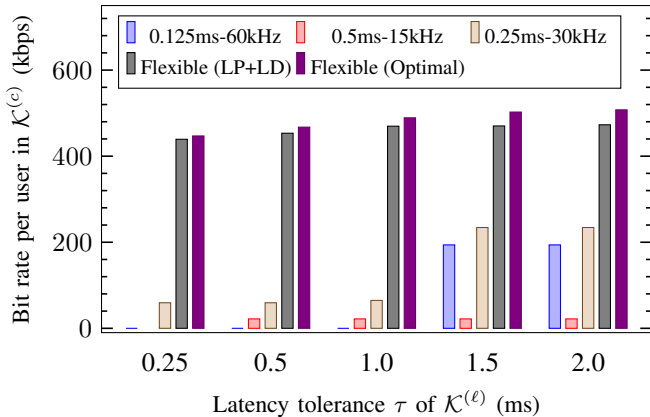


Figure 2. The figure shows bit rate of $\mathcal{K}^{(c)}$ with respect to latency tolerance τ of $\mathcal{K}^{(\ell)}$. The bit rate demand of $\mathcal{K}^{(\ell)}$ equals 128 kbps. All the three cases of non-flexible structures are solved to optimality. When $\tau = 0.25$, using the block 0.5ms-15kHz results in infeasibility.

Figure 3 shows the optimality gaps as function of the demand of $\mathcal{K}^{(\ell)}$. Here we also include $\text{BA}(\phi, r)$, which uses the throughput of each block-service pair as the utility. One can observe that in general the optimality gap increases with the user demand. Meanwhile, searching in the dual space for computing block-service utilities in most cases leads to significantly better results than considering the LP relaxation. With high user demand, $\text{BA}(\phi, r)$ and $\text{BA}(\mathcal{S}, \mathbf{u}_{LP})$ are clearly inferior to the others. Basically, using LD for utility estimation significantly reduces the optimality gap. In addition, combining $\text{BA}(\mathcal{S}, \mathbf{u}_{LP})$, $\text{BA}(\mathcal{S}, \mathbf{u}_{LD})$ leads to further optimality gap reduction, indicating that LP and LD are complementary to each other. Overall, the gap of LP+LD is below 10%.

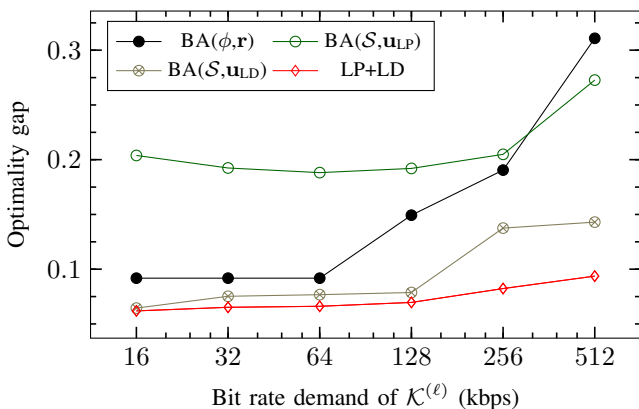


Figure 3. The figure shows the optimality gaps of the solutions obtained. For instance, “0.1” in the y-axis in Figure 3 means that the relative deviation to the optimum is 10% on average.

VI. CONCLUSION

We suggest that combining a flexible numerology and frame structure serves as a promising option for spectral efficiency. Utilizing LP and LD enables efficient problem solving.

ACKNOWLEDGEMENT

This work has been partially supported by European Union H2020 MSCA projects ACT5G (643002) and DECADE (645705), and the Center for Industrial Information Technology (CENIIT). The work of the first author was partly accomplished while he was at Linköping University, Sweden.

REFERENCES

- [1] B. Soret, P. Mogensen, K. I. Pedersen, and M. C. Aguayo-Torres, “Fundamental tradeoffs among reliability, latency and throughput in cellular networks,” in *IEEE Globecom Workshops*, 2014, pp. 1391–1396.
- [2] K. Pedersen, F. Frederiksen, G. Berardinelli, and P. Mogensen, “A flexible frame structure for 5G wide area,” in *IEEE VTC-Fall*, 2015, pp. 1–5.
- [3] G. Pocovi, B. Soret, K. I. Pedersen, and P. Mogensen, “MAC layer enhancements for ultra-reliable low-latency communications in cellular networks,” in *IEEE ICC Workshops*, 2017, pp. 1005–1010.
- [4] K. Pedersen, G. Pocovi, J. Steiner, and S. Khosravirad, “Punctured scheduling for critical low latency data on a shared channel with mobile broadband,” in *IEEE VTC-Fall*, 2017, pp. 1005–1010.
- [5] Q. Liao, P. Baracca, D. Lopez-Perez, and L. G. Giordano, “Resource scheduling for mixed traffic types with scalable TTI in dynamic TDD systems,” in *IEEE Globecom Workshops*, 2016, pp. 1–7.
- [6] E. Fountoulakis, N. Pappas, Q. Liao, V. Suryaprakash, and D. Yuan, “An examination of the benefits of scalable TTI for heterogeneous traffic management in 5G networks,” in *WiOpt*, 2017, pp. 1–6.
- [7] A. Anand, G. de Veciana, and S. Shakkottai, “Joint scheduling of URLLC and eMBB traffic in 5G wireless networks,” *arXiv.org*, Dec. 2017.
- [8] Y. Zhang and C. Leung, “Resource allocation in an OFDM-based cognitive radio system,” *IEEE Transactions on Communications*, vol. 57, no. 7, pp. 1928–1931, 2009.
- [9] T. Wang, H. Feng, and B. Hu, “Two-dimensional resource allocation for OFDMA system,” in *IEEE ICC Workshops*, 2008, pp. 1–5.
- [10] Y. Ben-Shimol, I. Kitroser, and Y. Dinitz, “Two-dimensional mapping for wireless OFDMA systems,” *IEEE Transactions on Broadcasting*, vol. 52, no. 3, pp. 388–396, 2006.
- [11] L. Zhang, A. Ijaz, P. Xiao, A. Qudus, and R. Tafazolli, “Subband filtered multi-carrier systems for multi-service wireless communications,” *IEEE Transactions on Wireless Communications*, vol. 16, no. 3, pp. 1893–1907, 2017.
- [12] A. A. Zaidi, R. Baldemair, H. Tullberg, H. Bjorkegren, L. Sundstrom, J. Medbo, C. Kilinc, and I. D. Silva, “Waveform and numerology to support 5G services and requirements,” *IEEE Communications Magazine*, vol. 54, no. 11, pp. 90–98, 2016.
- [13] P. Guan, D. Wu, T. Tian, J. Zhou, X. Zhang, L. Gu, A. Benjebbour, M. Iwabuchi, and Y. Kishiyama, “5G field trials: OFDM-based waveforms and mixed numerologies,” *IEEE Journal on Selected Areas in Communications*, vol. 35, no. 6, pp. 1234–1243, 2017.
- [14] A. Yazar and H. Arslan, “A flexibility metric and optimization methods for mixed numerologies in 5G and beyond,” *IEEE Access*, vol. 6, pp. 3755–3764, 2018.
- [15] A. Ijaz, L. Zhang, M. Grau, A. Mohamed, S. Vural, A. U. Qudus, M. A. Imran, C. H. Foh, and R. Tafazolli, “Enabling massive IoT in 5G and beyond systems: PHY radio frame design considerations,” *IEEE Access*, vol. 4, pp. 3322–3339, 2016.
- [16] 3GPP. (2017, Apr.) TS 36.101, Evolved Universal Terrestrial Radio Access (E-UTRA); User Equipment (UE) radio transmission and reception. Release 14. [Online]. Available: <http://www.3gpp.org>
- [17] M. Bataieri, K. Baum, and T. P. Krauss, “Cyclic prefix length analysis for 4G OFDM systems,” in *IEEE VTC-Fall*, 2004, pp. 543–547.
- [18] L. You, Q. Liao, N. Pappas, and D. Yuan, “2D resource allocation,” 2018. [Online]. Available: <http://dx.doi.org/10.21227/ch8e-x385>
- [19] S. Sen and H. D. Sherali, “A class of convergent primal-dual subgradient algorithms for decomposable convex programs,” *Mathematical Programming*, vol. 35, no. 3, pp. 279–297, 1986.
- [20] 3GPP TS 38.211, “NR; Physical channels and modulation,” Tech. Rep. V15.1.0, 2018.
- [21] J. Sachs, G. Wikstrom, T. Dudda, R. Baldemair, and K. Kittichokechai, “5G radio network design for ultra-reliable low-latency communication,” *IEEE Network*, vol. 32, no. 2, pp. 24–31, March 2018.
- [22] H. Miao and M. Faerber, “Physical downlink control channel for 5G new radio,” in *European Conference on Networks and Communications*, 2017, pp. 1–5.
- [23] X. Zhang, M. Jia, L. Chen, J. Ma, and J. Qiu, “Filtered-OFDM - enabler for flexible waveform in the 5th generation cellular networks,” in *IEEE GLOBECOM*, 2015, pp. 1–6.